Background oriented schlieren demonstrations

Final report for the European Research Office
Edison House
223-231 Old Marylebone Road
London NW15TH, United Kingdom

R+D 8963-AN-01S

Contract No. N68171-00-M-5854

Professor Meier

H. Richard **M. Raffel**

Deutsches Zentrum für Luft- und Raumfahrt e.V.
10 Bunsenstrasse
37073 Göttingen
Germany

In cooperation with

C. Burley **K. Kinzie**

NASA Langley Research Center
100 NASA Road
Hampton, VA 23681-2199

Y. Yu **Chee Tung**

Aeroflightdynamics Directorate
Moffett Field, CA 94035

Abstract

In this project report we present the application of a novel schlieren technique for two different tests. The optical method is referred to as "Background Oriented Schlieren" (BOS) in the following. Additionally the differences between BOS and an extension of it, the reference-free stereoscopic arrangement (BOSS in the following), will be discussed. Experimental studies have been carried out to investigate a supersonic jet in an anechoic chamber of Nasa Langley and details of the vortex generation next to the blade tips of an Sikorsky UH60 of AFDD at Ames. The background oriented techniques seem to well complete other optical techniques like shadowgraphy or focussing schlieren methods and yield additional quantitative information. Furthermore, they allow - in contrast to laser based techniques - to study the Reynolds-number depending vortex development in full-scale flight tests more easily.

The aim of this paper is not to describe the optical measurement technique in detail, this can be found in other publication, (Raffel et al 2000, Richard et al. 2000 and Meier 2000), but to show the quality and kind of information that can be expected by the example of helicopter flight investigations. Additional tests at a supersonic nozzle have been performed in order to get more quantitative results in contrast to the helicopter tests where the study of the feasibility was the major goal.

The motivation for the helicopter investigations shall shortly be outlined in the following. After that, an overview over the BOS technique will be given and sample data will be shown further down. The complete data sets for the quantitative tests of the jet flow – approximately 12 Gigabyte – and the evaluated results of the in-flight feasibility study – approximately 400 Megabyte – have been handed out to the partners on CD and tape during the HART II meeting in the Netherlands September 2000.

Introduction

With increasing use of civil helicopters, the problem of noise emission of helicopters has become increasingly important within the last decades. Blade vortex interactions (BVI) have been identified as major responsible for the acoustic nuisance which occurs especially during low speed descending flight conditions like landing approach or maneuvers. Moreover, the interactions affect blade loads and rotor performance. Therefore, many aeronautical research organizations develop and run numerical codes in order to predict the rotor wake (see e.g. Beaumier et al. 1994). These aerodynamic results can then be used for further numerical investigations of the acoustic near and far field of BVI. (e.g. Burley et al. 1991, Ehrenfried et al. 1991).

Theoretical and experimental studies were conducted in order to validate models for predicting BVI and to determine the model-to-full-scale acoustic scaling conditions (Schlinker and Amiet 1983, Splettstößer et al. 1984) and generally confirmed the necessity of wind tunnel tests. It has been found that high speed noise at the advancing blades can be quite well scaled whereas the scalability of BVI noise underlies certain restrictions. It is assumed that Reynolds number effects do not allow to scale the vortex dimensions easily. Therefore, aerodynamic rotor model investigations have been undertaken at large scales e.g. in the large low speed facility of the Dutch-German wind tunnel DNW-LLF (e.g. Splettstößer et al. 1997)

By reviewing the literature of the last decade, it can be seen, that particle based flow velocity measurements have most frequently been applied (e.g. Sullivan 1973, Biggers and Orloff 1974, Raffel et al. 1998). Most likely, because they are assumed to deliver a lot of quantitative information needed for BVI prediction.

Density measurements of the BVI phenomena on the other hand are also desirable, because the vortices under investigation are compressible and density gradient techniques can therefore be used in order visualize flow structures. Density measurements have been performed quite frequently, but mostly in two-dimensional basic investigation (e.g. Meier et al. 1998, Chandrasekhara 1994). Density gradient visualization by the classical schlieren method as e.g. conducted by Tangler (1977) and were reported more recently by Bagai and Leishman (1993). For large or full–scale investigations on rotating systems, the traditional quantitative density techniques like Mach-Zehnder or point diffraction interferometry seem to bee less feasible, since they require delicate optical systems. Due to the aforementioned reason of limited scalability and the well known imperfections of particle based optical techniques to resolve the vortex core in detail and their costs, additional large or full scale tests of an easy to use optical technique are desirable.

Background Oriented Schlieren (BOS) technique

The principle of this optical technique used for our studies is based on the refractive index variation of air due to density gradients. The relation between density gradients and refractive index variations is given by the Gladstone-Dale equation:

$$\frac{n-1}{\rho} = G(\lambda)$$

with n: refractive index
ρ: density ($kg \times m^{-3}$)
$G(\lambda)$=Gladstone-Dale number

where $G(\lambda)$ is defined by:

$$G(\lambda) = 2.2244 \times 10^{-4} \cdot \left(1 + \left(\frac{6.7132 \times 10^{-8}}{\lambda}\right)^2\right)$$

with λ: wave length (m)

The technique can best be compared with the density speckle photography as described by Debrus et al. (1972), Köpf (1972), and in an improved version by Wernekinck and Merzkirch (1987).

In contrast to laser speckle velocimetry, where speckle patterns are generated by a double exposure of highly seeded flows, in the density speckle photography, speckle patterns are generated by a ground glass in order to obtain density gradient information. Like interferometry, the density speckle photography uses an expanded parallel laser beam, which is shining through a transonic flow field or - in more general terms - through an object containing refraction index changes. However, in contrast to interferometry, speckle patterns are generated instead of interference fringes.

In a first step a reference image is generated by a recording of a speckle pattern observed through air at rest before the experiment. An additional exposure observing the speckle pattern through the flow under investigation (i.e. during the wind tunnel run) leads to a second image. The resulting images of both exposures can then be evaluated by correlation methods. In other words, without further evaluation efforts, algorithms, which have been developed and optimized e.g. for particle image velocimetry (or other forms of speckle photography) can now be used to determine speckle displacements. It can easily be shown, that the deflection of a single beam contains information about the spatial gradient of the refractive index integrated along the optical path. Assuming paraxial recording and small deflection angles a formula for the image displacement Δy_i can be derived, which is valid for density speckle photography as well as for the Background Oriented Schlieren technique which we used:

$\Delta y_i = Z_D M \varepsilon$

with: $M = z_i / Z_B$ ~ magnification factor
Z_D ~ distance dot pattern - density gradient
ε is defined by:

$$\varepsilon = \frac{1}{n_0} \int_{Z_D - \Delta Z_D}^{Z_D + \Delta Z_D} \frac{\delta n}{\delta y} dz$$

The deflection of the beams causes a displacement of the speckle patterns with respect to the patterns of the reference recording, which can be interpreted as density gradients – integrated along the optical path - by using the Gladstone-Dale equation. It is obvious, that from the two dimensional density gradient an estimate for the density itself can be obtained by integration. After this, the result is comparable to x-ray images and like them, they can be recorded and evaluated employing tomographic methods. However, for the speckle method this would not only require multiple cameras, but also multiple sending optics to form and direct the beams passing through the object under investigation.

The main difference between the background oriented optical technique proposed in this article and the other methods mentioned above is, that the BOS method does not require any optical devices on the sending side. The only optical part needed is an objective lens mounted for instance on a video camera on the receiving side. The camera used is focused on a random dot pattern in the background, which generates an image quite similar to a particle image or a speckle pattern. For this reason we refer to this approach to be "background oriented". The flow field under investigation is located on the viewing axis. Due to the refractive index gradients the dot pattern will be displaced with respect to the reference recording when observing it on the recording side (see Fig. 1).

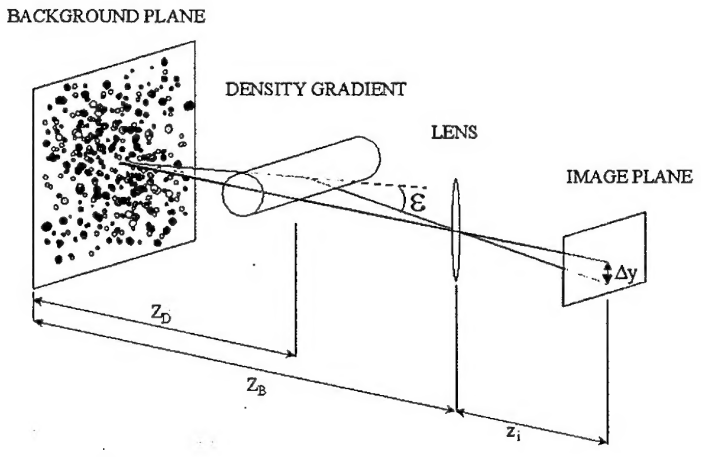

Fig. 1: Optical path for density gradient measurements by light deflection

When looking at the BOS approach, it seems to be identical to the density speckle photography. However, two major differences can be noticed: First, instead of a laser and beam expanding optics, any background of sufficient contrast and spatial frequency, for example a print-out of a random dot pattern, and white light can be used. This results in significantly reduced efforts during the application of the BOS technique. Second, the optical paths over which the density effects are averaged are divergent with respect to each other. This can result in a clear disadvantage when large viewing angles have to be used, but is of little influence for recording distances of more than 30 meters as used for the helicopter tests described in this paper. For a later extension towards "Background Oriented Optical Tomography" (BOOT), which has been proposed by G.E.A. Meier (Meier 1999), the divergence of the optical paths should be no problem since convolution methods for divergent beams are already known and described in the literature (see e.g. Herman 1980).

Stereoscopic BOSS method for reference evaluation

The previously described BOS technique can be extended by using two cameras simultaneously in a stereoscopic configuration. Both cameras are looking onto the same background through the flow under investigation (see Fig. 2). Due to the different camera positions, the images of the background pattern are not at the same position in the sensor plane of each camera. Thus, the two resulting images can be cross-correlated with each other. The image of one camera can be defined as a reference for the other one and vice-versa.

The advantage of this extension is that now no reference image has to be taken at a different time. This makes the technique better suitable for moving objects. In case of the helicopter in flight, two cameras can be very easily installed aboard, looking through the blade and focused on a far distance background which only must offer sufficient contrast. This concept is referred to as the reference-free BOSS technique in the following.

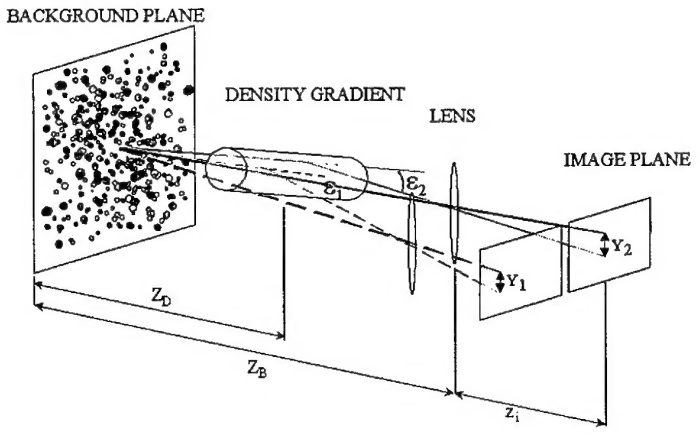

Fig. 2: Optical path with a setup for two cameras

Measurements of velocity and density with the PIV-BOS-system at Langley

Laboratory measurements with the BOS technique were planed and finally performed at Nasa Langley in order to get in sights into the accuracy of the technique. PIV two-component measurements and three-component stereoscopic measurements have been performed at the exit of a two-inch nozzle at three different Mach numbers. The recording system consisted of two cameras connected to one mobile PC, which has been used for data storage and operation of the acquisition and evaluation software for PIV and BOS. In order to allow a later quantitative comparison the same set of parameters has been measured by PIV and BOS within a two days test.

Particle Image Velocimetry (PIV) measurements:

In the following the small jet flow facility of the aeroacoustic branch at Nasa Langley can bee seen. The Laser system used was a Spectron PIV 400 system which contains of two double of two Nd:YAG laser resonators with frequency doubler. The pulse energy used was approximately 300 mJ at 532 nm.

Fig 3: pictures of the PIV setup

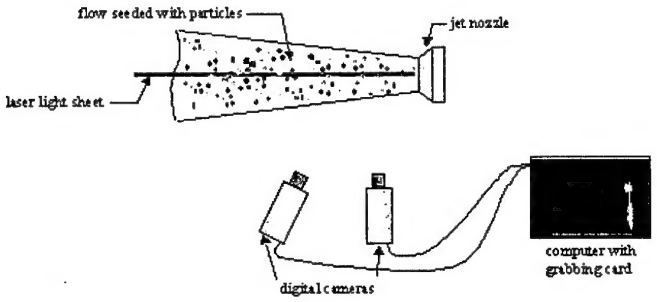

Fig 4: sketch of the PIV setup

The recording has been done with the following parameterers:

Mach number	NPR	Δt between the 2 pulses
0.5	1.186	5μs
0.85	1.604	3μs
1.09	2.1	2μs

Tab. 1: Test matrix

The Flow seeding inside the jet flow has been done with a small Laskin nozzle atomizer with limited performance. Therefore the particle density changed depending on the mass flow rate and the entrainment of surrounding fluid.

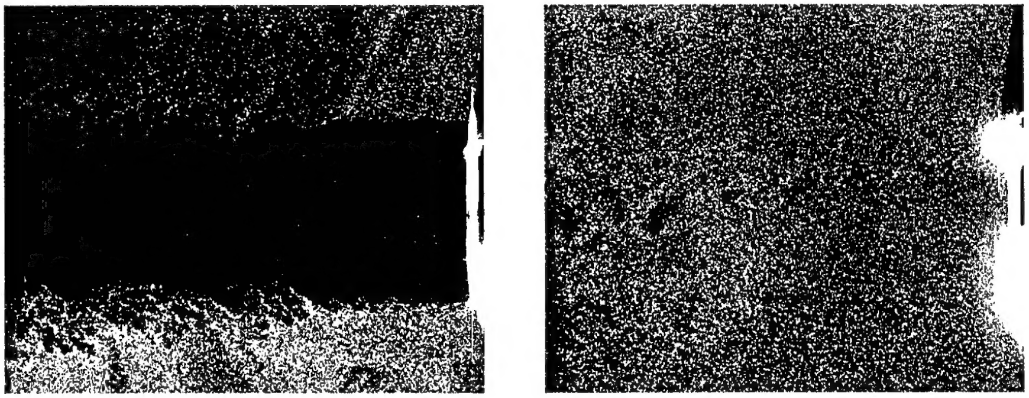

Fig 5: examples of PIV pictures at mach=0.85 (left: without tab, right: with tab)

Two-component PIV measurements

Instantaneous and averaged sample data of two-component PIV measurements are shown in the following.
Measurements without tab:

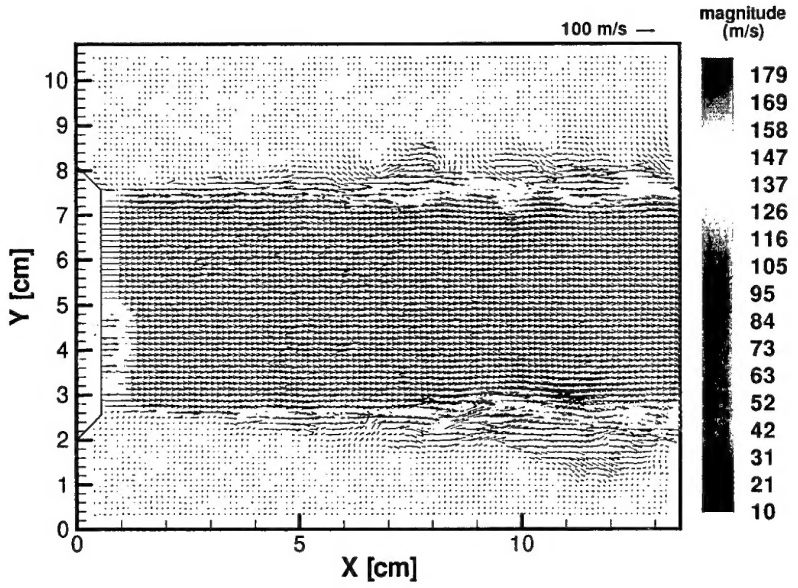

Fig 6: Instantaneous velocity and magnitude fields: mach=0.5
(windows size=24 pixels, step size=12 pixels)

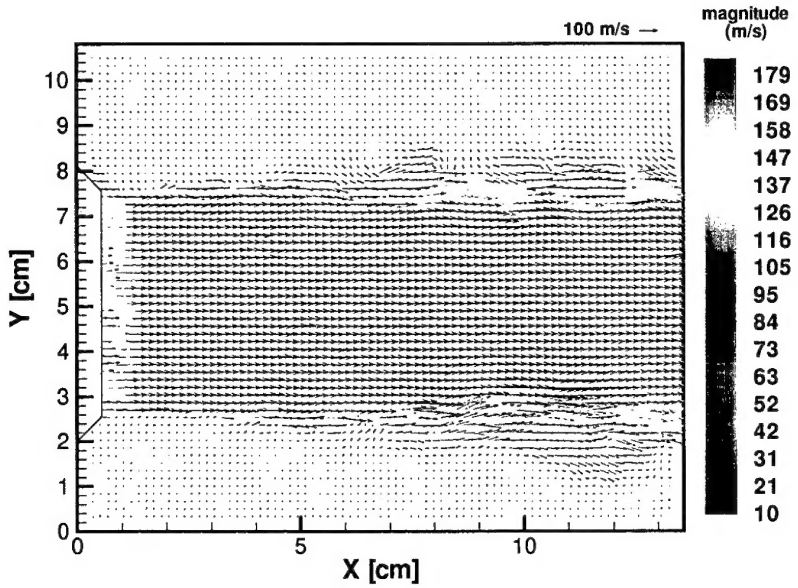

Fig 7: Instantaneous velocity and magnitude fields: mach=0.5
(windows size=32 pixels, step size=16 pixels)

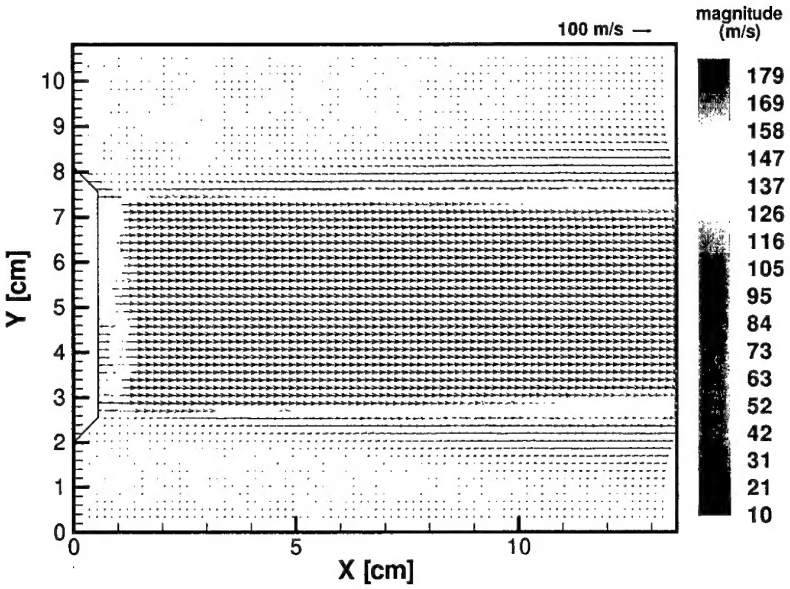

Fig 8: Averaged velocity and magnitude fields: Mach No. = 0.5
(windows size=32 pixels, step size=16 pixels)

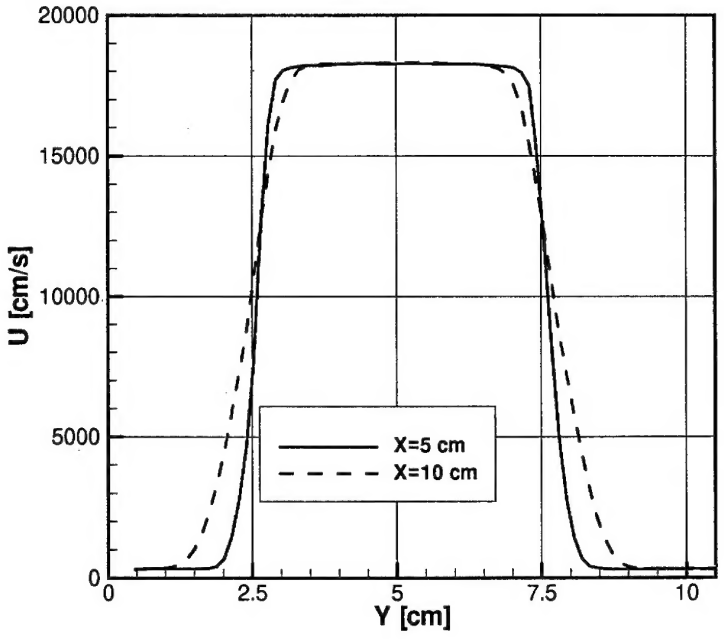

Fig 9: Extracted velocity lines from the previous result for x=5 and x=10 cm

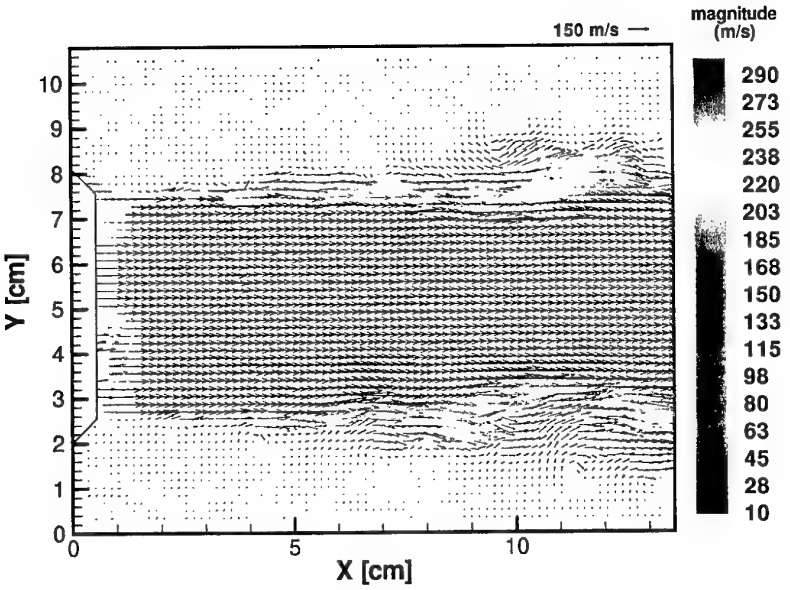

Fig 10: Instantaneous velocity and magnitude fields: Mach No. = 0.85
(windows size=32 pixels, step size=16 pixels)

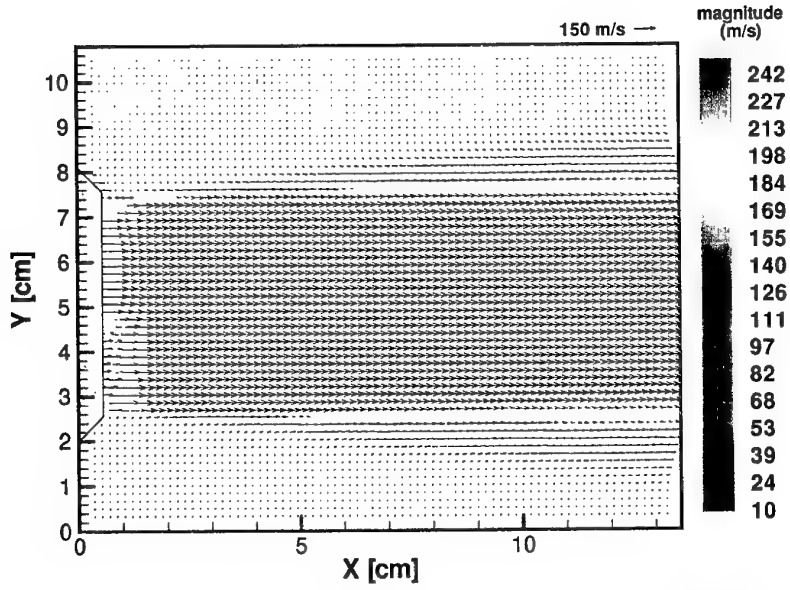

Fig 11: Averaged velocity and magnitude fields: Mach No. = 0.85
(windows size=32 pixels, step size=16 pixels)

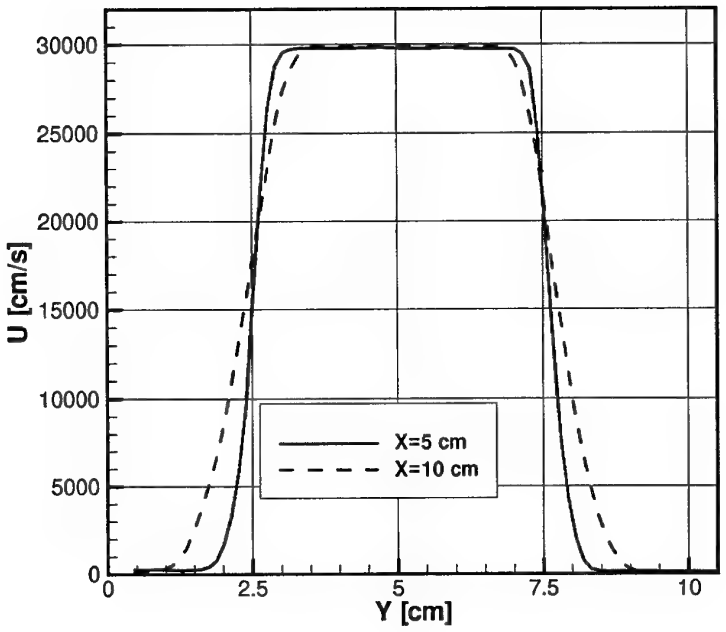

Fig 12: Extracted velocity lines from the previous result for x=5 and x=10 cm

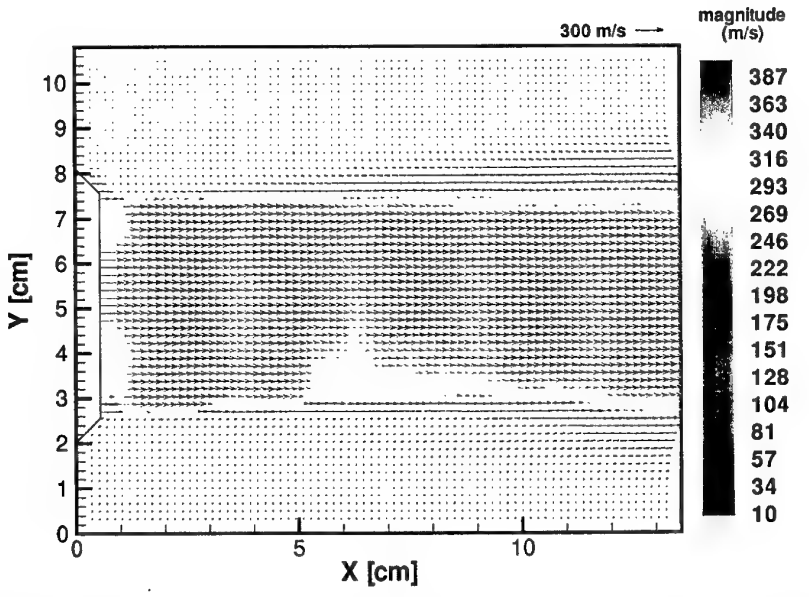

Fig 13: Averaged velocity and magnitude fields: Mach No. = 1.09
(windows size=32 pixels, step size=16 pixels)

Measurements with tab:

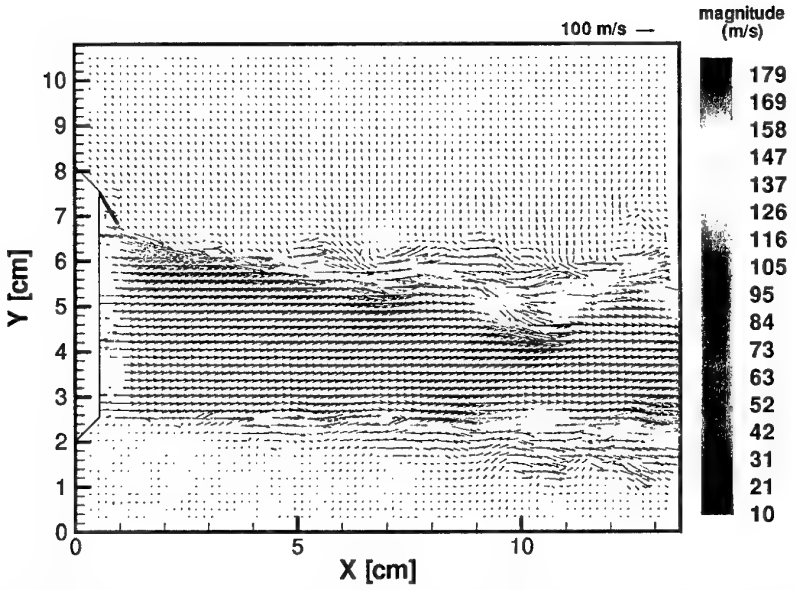

Fig 14: Instantaneous velocity and magnitude fields: Mach No. = 0.5
(windows size=32 pixels, step size=16 pixels)

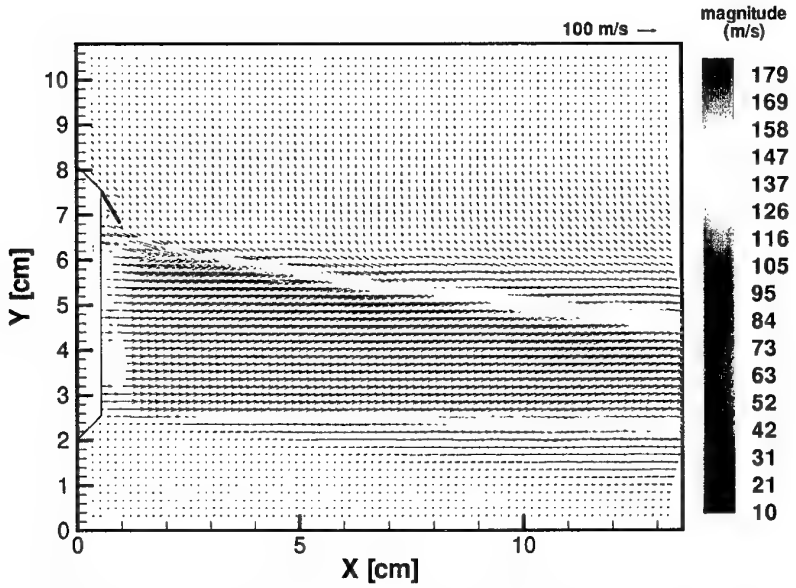

Fig 15: Averaged velocity and magnitude fields: Mach No. = 0.5
(windows size=32 pixels, step size=16 pixels)

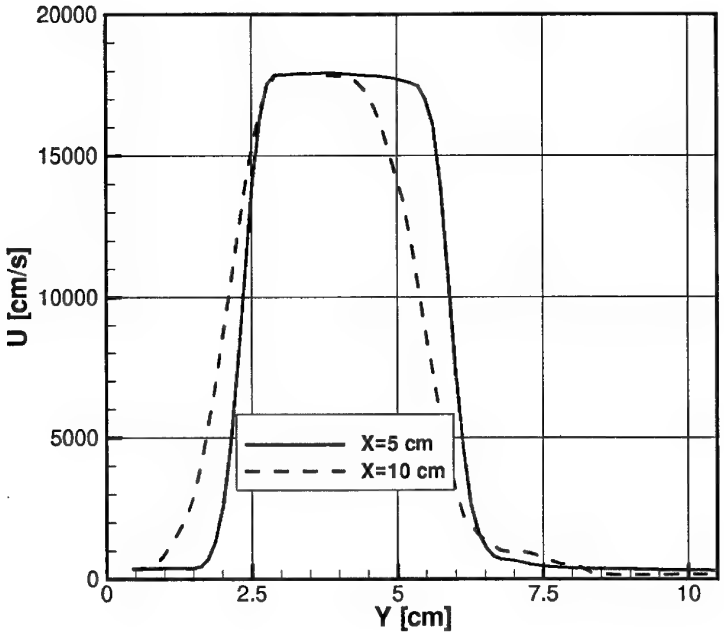

Fig 16: Extracted velocity lines from the previous result for x=5 and x=10 cm

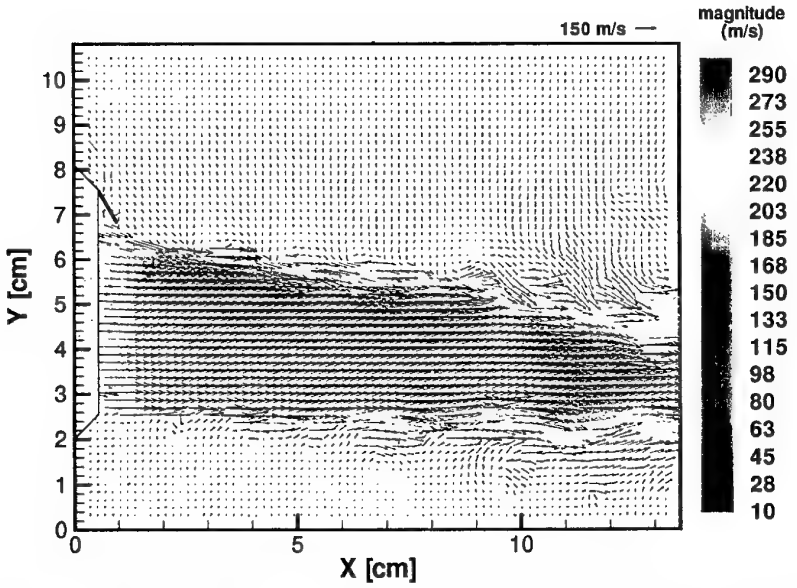

Fig 17: Instantaneous velocity and magnitude fields: Mach No. = 0.85
(windows size=32 pixels, step size=16 pixels)

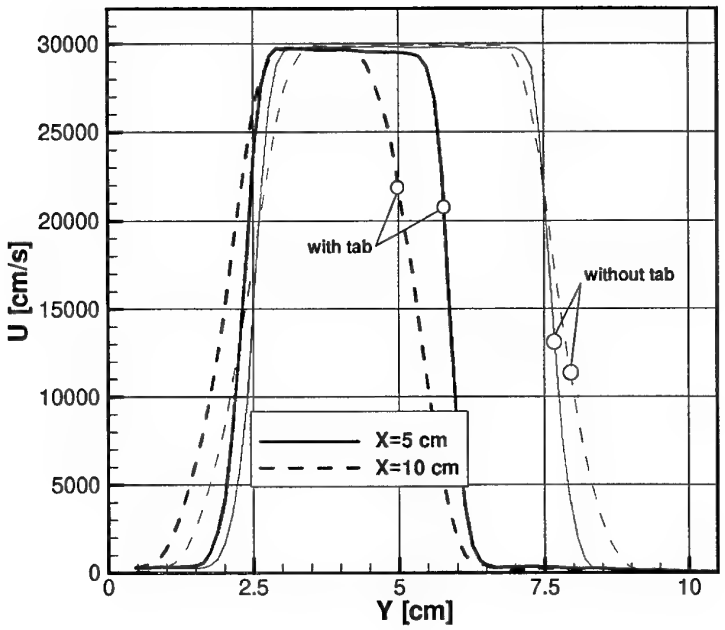

Fig 18: Extracted velocity lines for x=5 and x=10 cm
with and without tab for Mach No. = 0.85

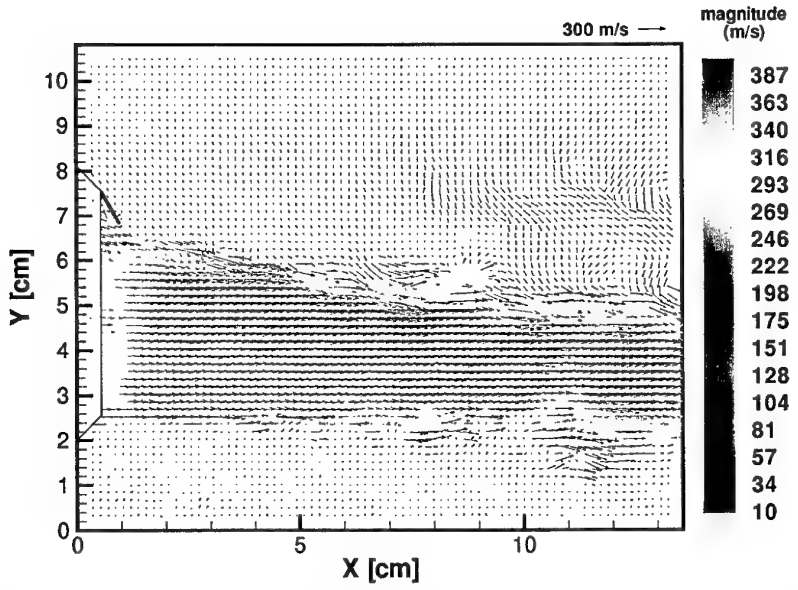

Fig 19: Instantaneous velocity and magnitude fields: Mach No. = 1.09
(windows size=32 pixels, step size=16 pixels)

Three-component PIV measurements

Stereoscopic PIC requires the dewarping of the evaluated displacement data or – and this is the way which has been done here – the dewarping of the raw image data. The calibration recording and the resulting transformation coefficients are shown below. The calibration procedure and the subsequent dewarping has been described in detail by Raffel et al. (1998)

List of the dewarping coefficients used for all image data.

Left dewarping coefficients

a00 = 0.769758
a01 = -0.0174591
a03 = 463.407
a10 = 0.0347116
a11 = 0.869413
a13 = 26.3604
a30 = 5.66924e-05
a31 = -5.0474e-06
a33 = 1
magnification = 1
rotation = 0
im_x_offset = 0
im_y_offset = 0
obj_x_offset = -180
obj_y_offset = -9

Right dewarping coefficients

a00 = 1.05892
a01 = 0.00222777
a03 = 1.23963
a10 = 0.00225538
a11 = 1.05599
a13 = 15.6272
a30 = 6.55742e-06
a31 = 2.36381e-07
a33 = 1
magnification = 1
rotation = 0
im_x_offset = 0
im_y_offset = 0
obj_x_offset = -180
obj_y_offset = -9

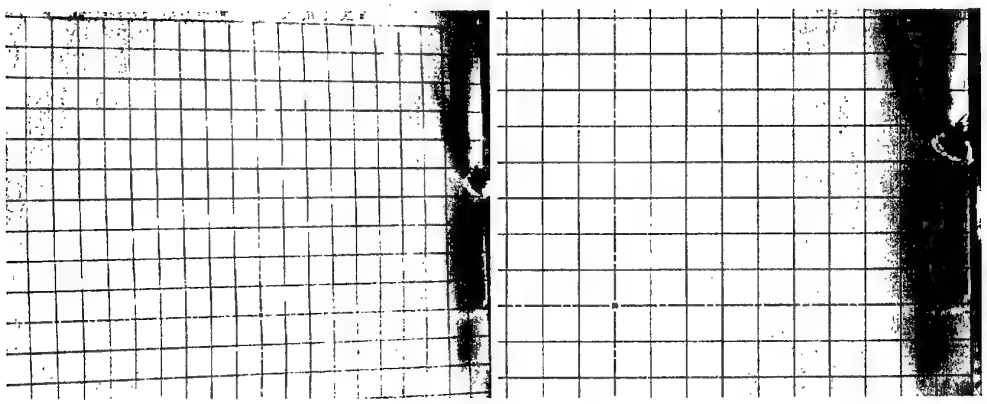

Fig 20: Left and right calibration grid picture before dewarping

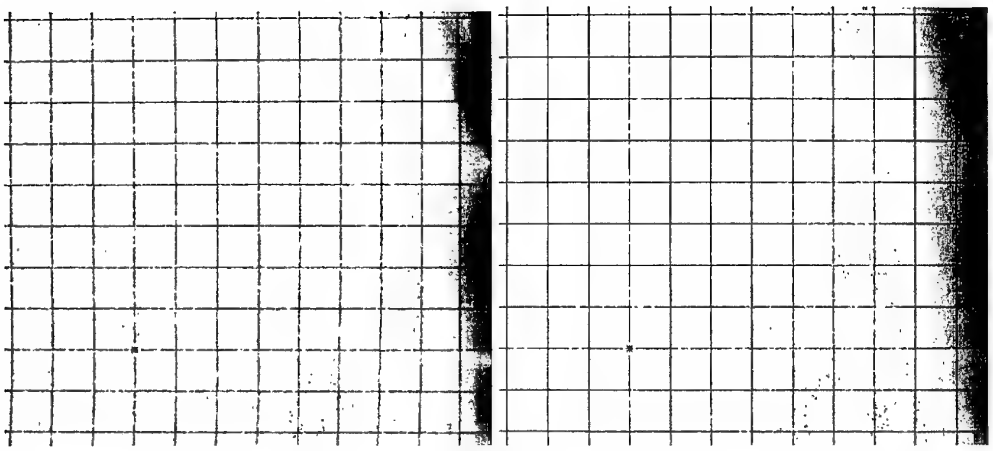

Fig 21: Left and right calibration grid picture after dewarping

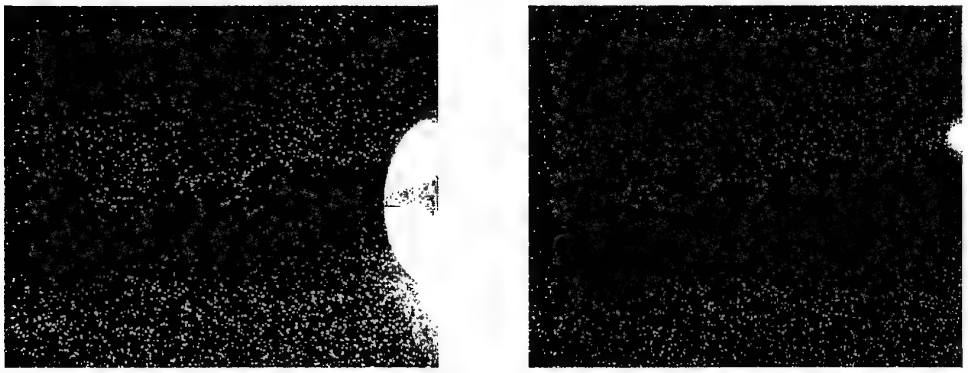

Fig 22: Example of dewarped PIV pictures from the left and right cameras

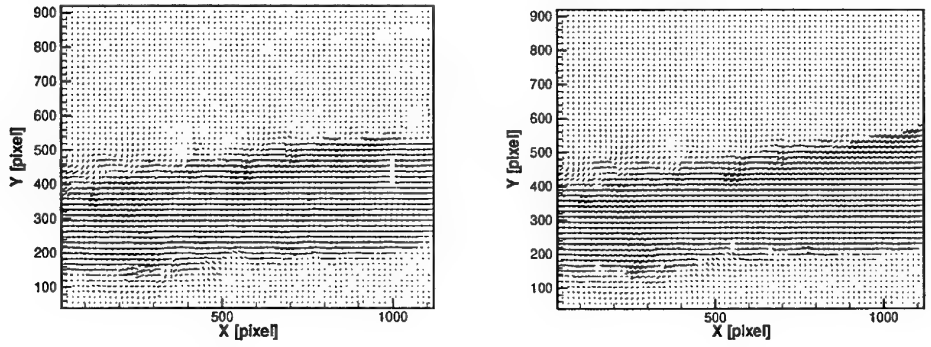

Fig 23: 2C-PIV results from the previous pictures (flow from right to left)

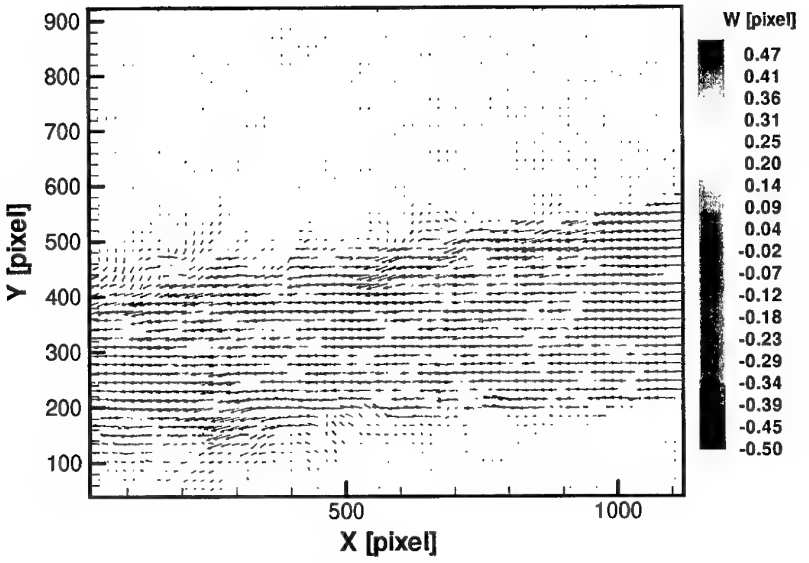

Fig 24: 3C-PIV results from the previous pictures (flow from right to left)

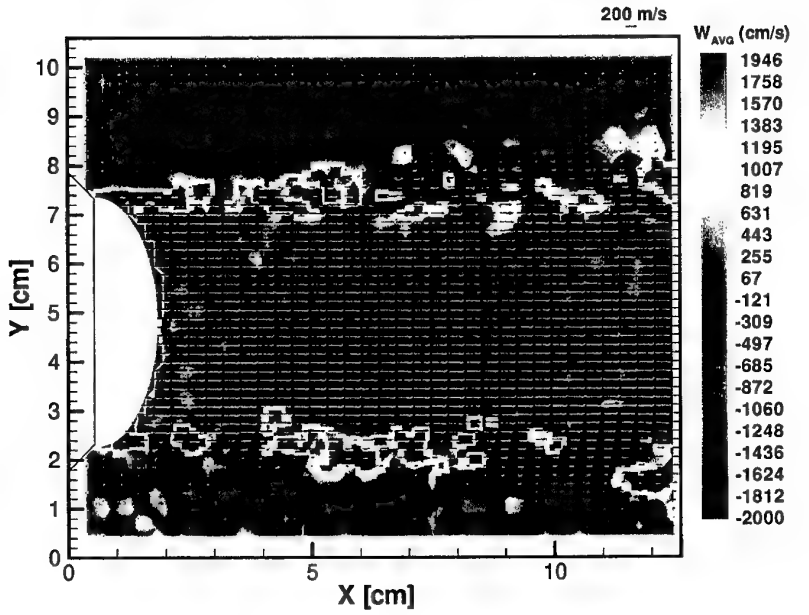

Fig 25: Averaged vector field for Mach No = 0.85 without tab (flow from left to right)

BOS measurements at Langley

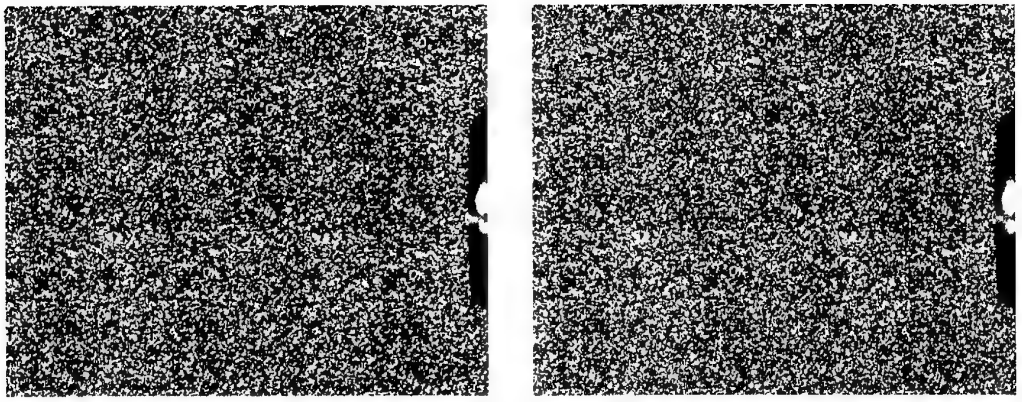

Fig 26: Reference picture (left) and picture with flow (right)

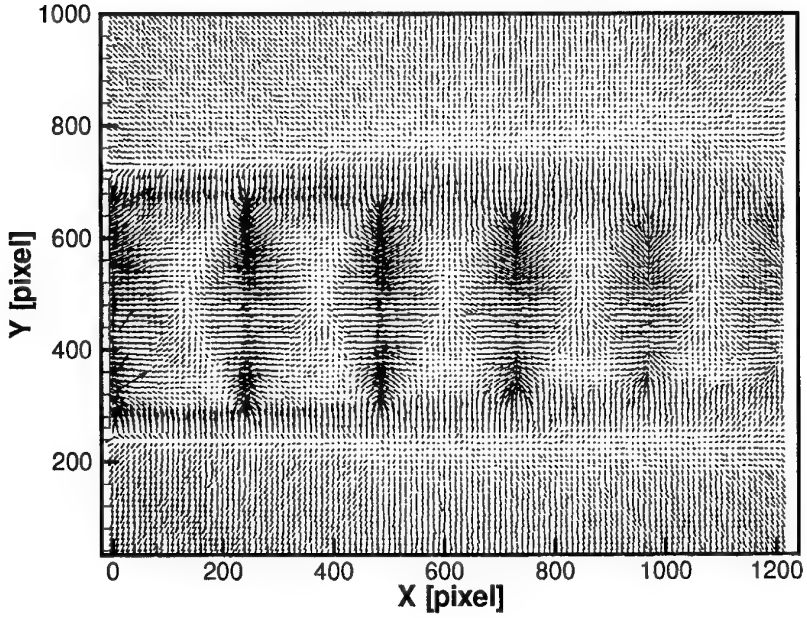

Fig 27: Vector field proportional to the density gradients

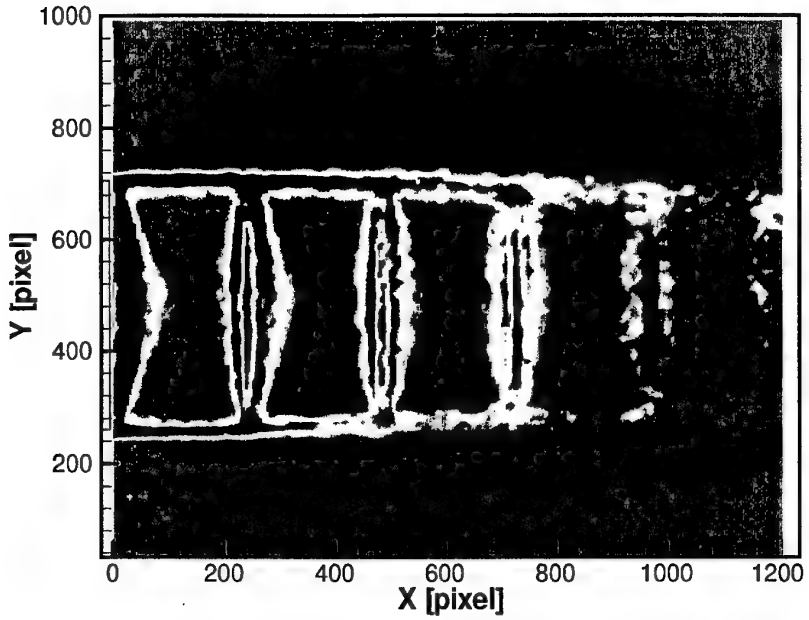

Fig. 28: Color coded density gradient distribution

A density distribution can be derived from the displacement (density gradient) field as shown in the following figures. It has been computed by integration along vertical (first plot, Fig. 29) and by vertical and horizontal lines (second plot, Fig. 30), which is the simplest method but produces line noise. This distribution can also be derived using the Poisson equation but this method had the disadvantage to strongly smooth the result.

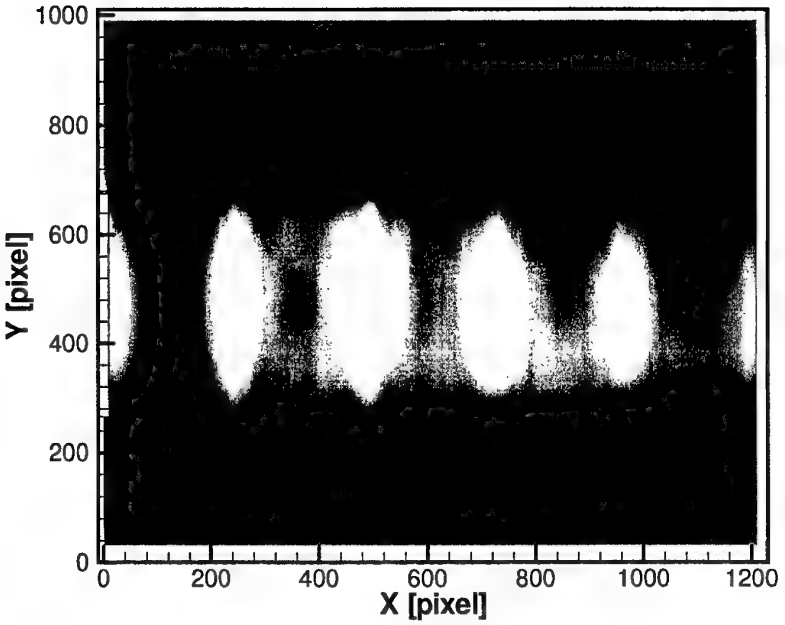

Fig. 29: Grey level plot proportional to density derived by vertical integration

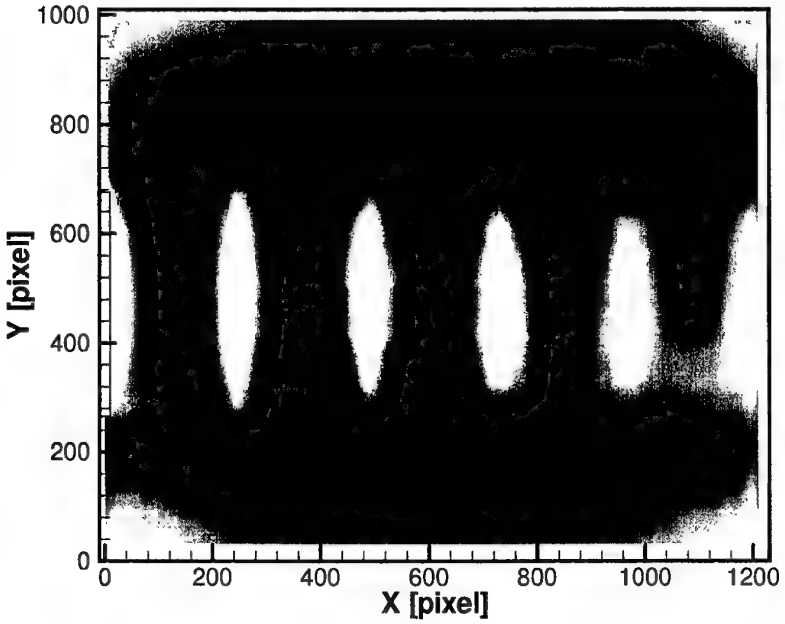

Fig. 30: Grey level plot proportional to density (vertical + horizontal integration)

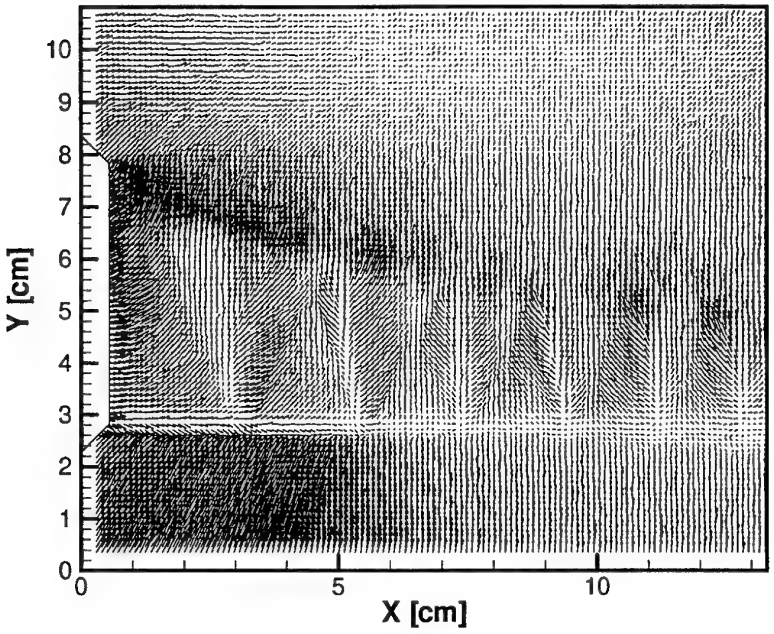

Fig 31: BOS : Mach No.=1.09 with tab (windows size=20 pixels, step size=10 pixels)

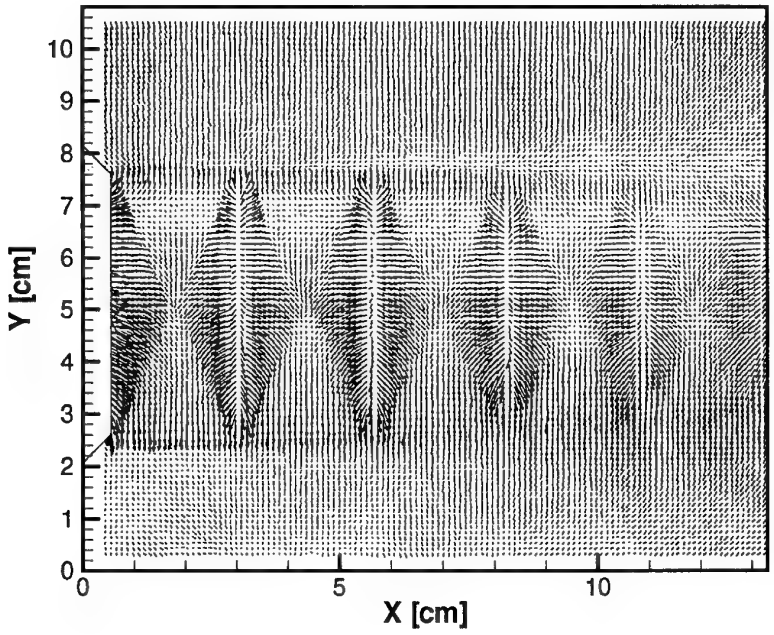

Fig 32: BOS : Mach No=1.09 without tab
(windows size=20 pixels, step size=10 pixels)

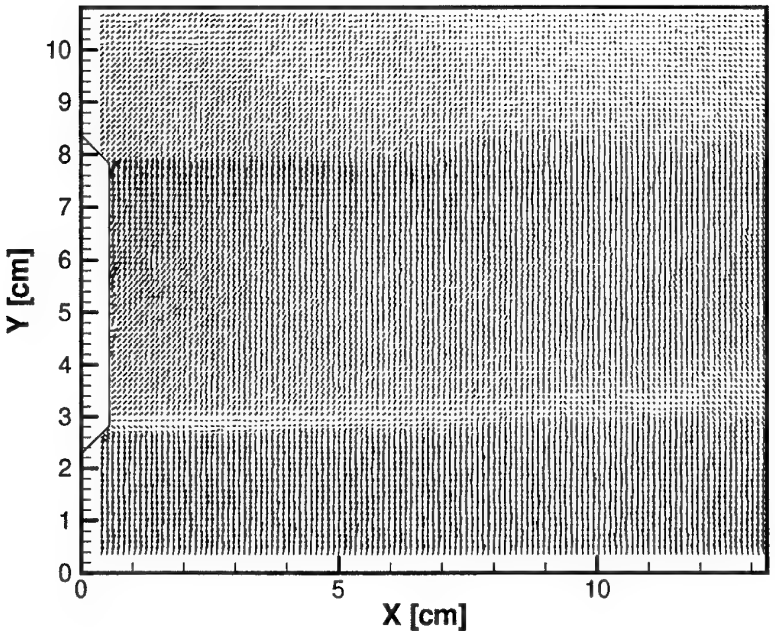

Fig 33: BOS : Mach No.=0.85 without tab
(windows size=20 pixels, step size=10 pixels)

Application of BOS to a helicopter in flight

Further tests have been performed very recently in a close cooperation between the aeromechanic Branch of the US Army and DLR at NASA Ames research center. The tests here were focussed on the structure of the tip vortices immediately after generation in the vicinity of the blade. The background of those investigations is the need to identify and localize the structure and center of the blade tip vortices in order to model and predict there interaction with the following blades. Complex tip geometries are frequently used in order to displace the vortices with respect to the tip path plane and to reduce the velocity gradients of the vortices by generating vortices of larger core sizes. Those tip geometries are mostly used on large and heavy helicopters, because the BVI noise amplitude increases with increasing air loads on the blades. Since larger helicopters require larger observation distances and the spatial resolution relative to the blade tip size had to be increased, the tests at Ames were quite challenging compared to the tests described in the previous section.

The equipment used were again the DLR's PIV cameras. In this case they were connected to a mobile computer system and equipped with different long focal lenses. A random dot pattern was again generated by splashing tiny droplets of white wall paint, but in a second test an grass area approximately 100 meters behind the helicopter has also successfully been used as a 'background pattern'.

The recording

The subject, a helicopter – UH 60 from Sikorsky – was investigated during a hover flight above the taxi way of the air field of Nasa Ames. Two progressive scan CCD cameras have been mounted in a window of a building in a horizontal distance of ~45 meters from the helicopter and 15 meters above the ground (see Fig. 34). The two cameras used belong to DLR's PIV equipment and have a 1024 x 1280 pixel resolution. They were closely spaced mounted (63 cm spaced) in order to try different magnifications of the same dot pattern simultaneously and were synchronized with a trigger signal of 3 Hz. A 100 mm lens and a 180 mm lens were mounted and directed to the same area on the ground. A random dot pattern was generated by splashing tiny droplets of white wall paint with a brush onto the concrete ground.

The reference recordings were made directly before the arrival of the helicopter.

Fig. 34: Photo of the cameras positions

Fig. 35: Photo of the UH60 in hover flight

The evaluation

Even if acceptable results could be obtained by using standard cross-correlation displacement measurement software, as developed for PIV, more sophisticated programs helped to adapt the peak-fitting routine to the size of the dot images. Finally we obtained the best result by using iterative Levenberg-Marquardt fit to a 10x10 pixel area, where the correlation values are weighted according to the Fisher transform (for details see Ronneberger et al. 1998). The size of the interrogation window was 40 by 40 pixels searched in a window of 64 x 64 pixels. The evaluation led to the vector plots shown in the following figures, they have been obtained by a massive oversampling using a 10 pixel step-width resulting in an improved visibility of the flow structures under investigation.

In the following figure the young vortex shedding from the blade that just passed the observation area – trailing edge visible on the right hand side – can easily be detected. It is located nearly directly on the blade tip path, which we were able to reconstruct from different recordings. The elliptical shape of the path is due to the underlying projection.

The results of the flight test at Ames

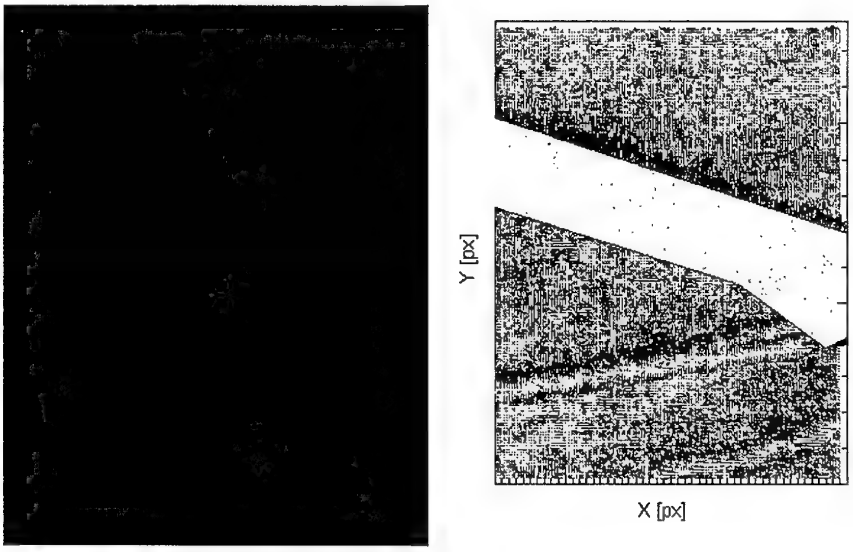

Fig. 36: Raw image from transonic blade tip over the background pattern (white dots on grey concrete) and the according density gradient plot with color coded gradient magnitude.

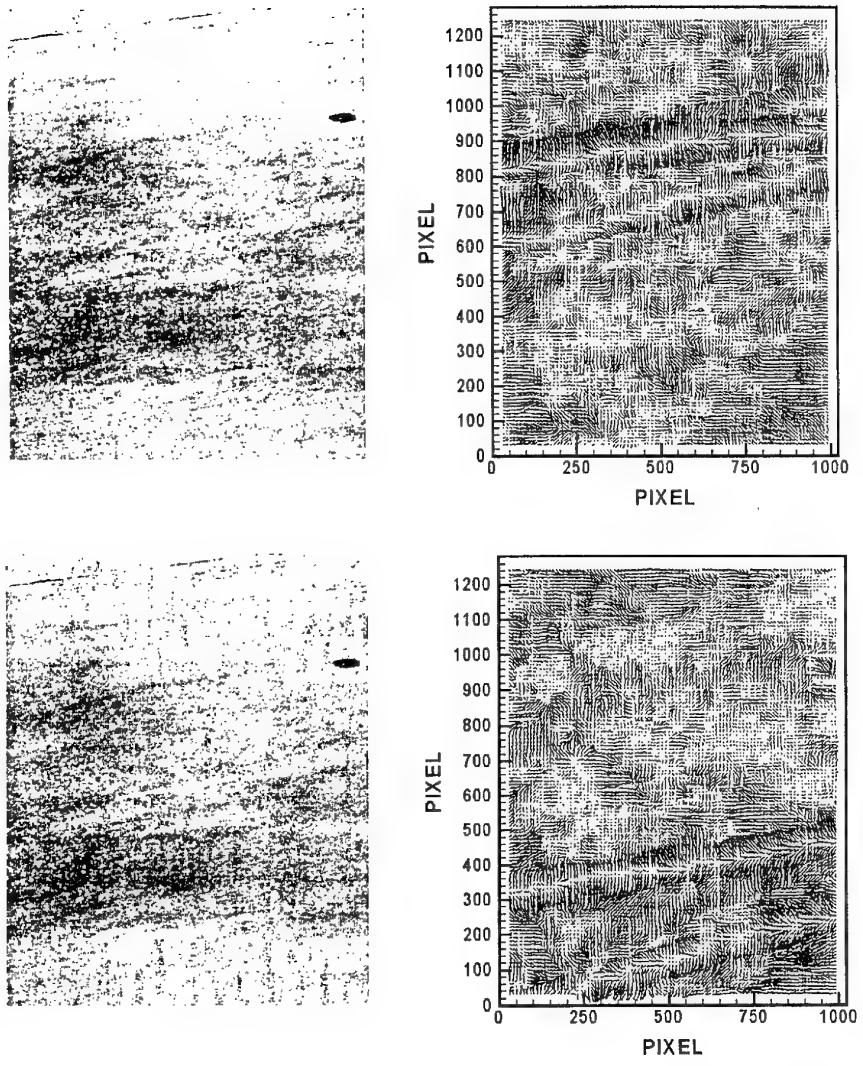

Fig. 37: Raw images from transonic blade tip over the background pattern (white dots on grey concrete) and the according density gradient plots

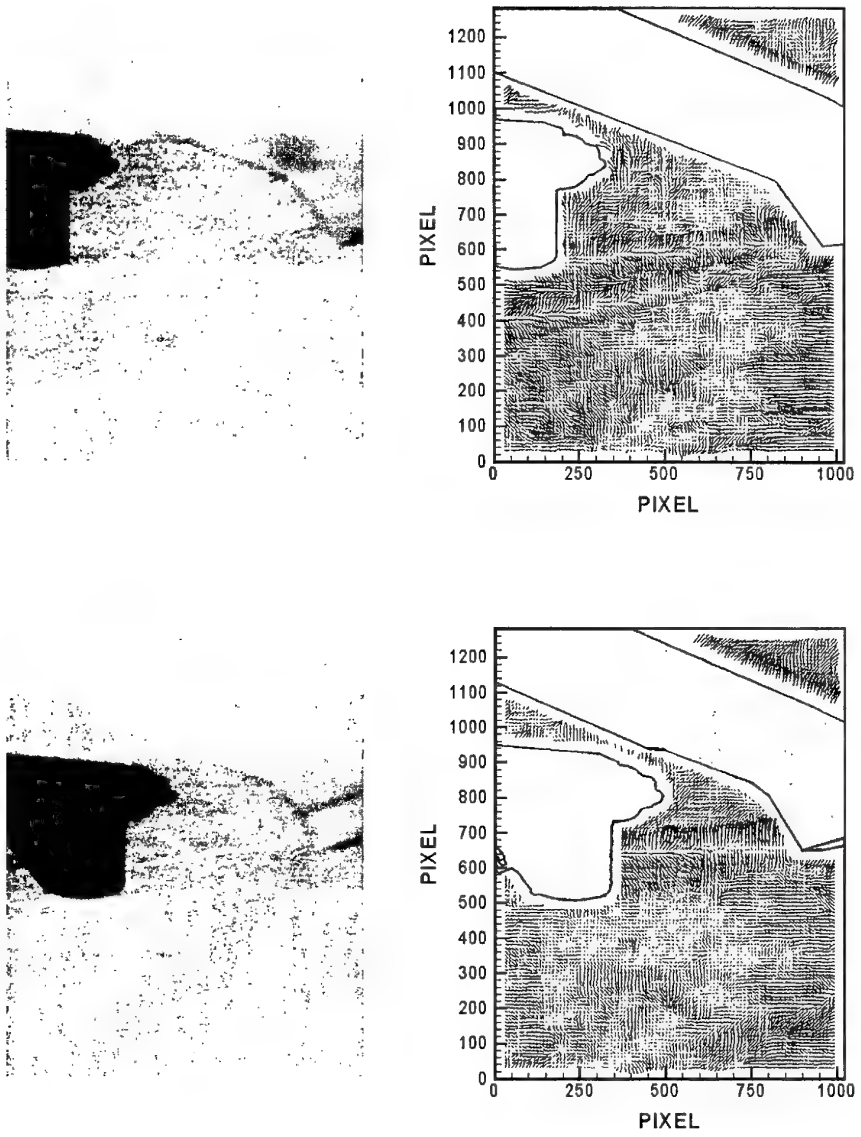

Fig. 38: Raw images from transonic blade tip over the background pattern (white dots on grey concrete) and the according density gradient plots

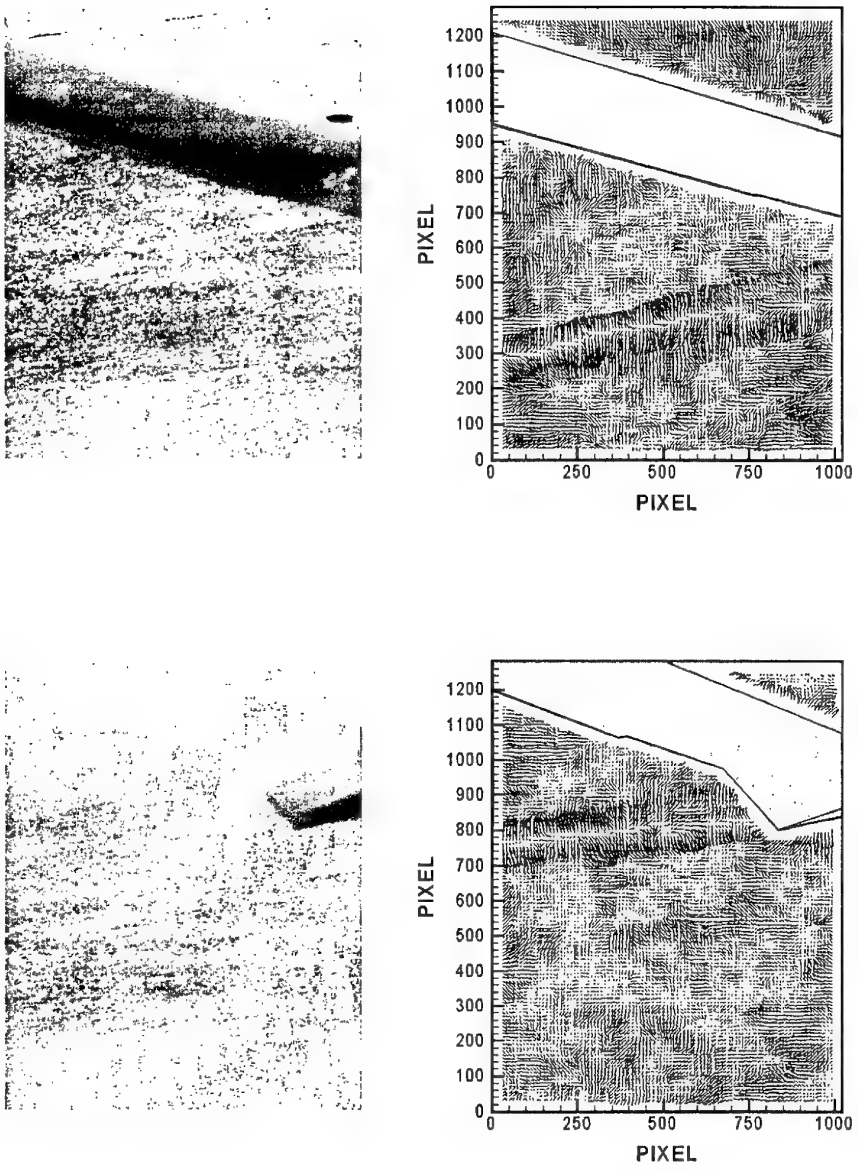

Fig. 39: Raw images from transonic blade tip over the background pattern (left side: auxiliary wings) and the according density gradient plots

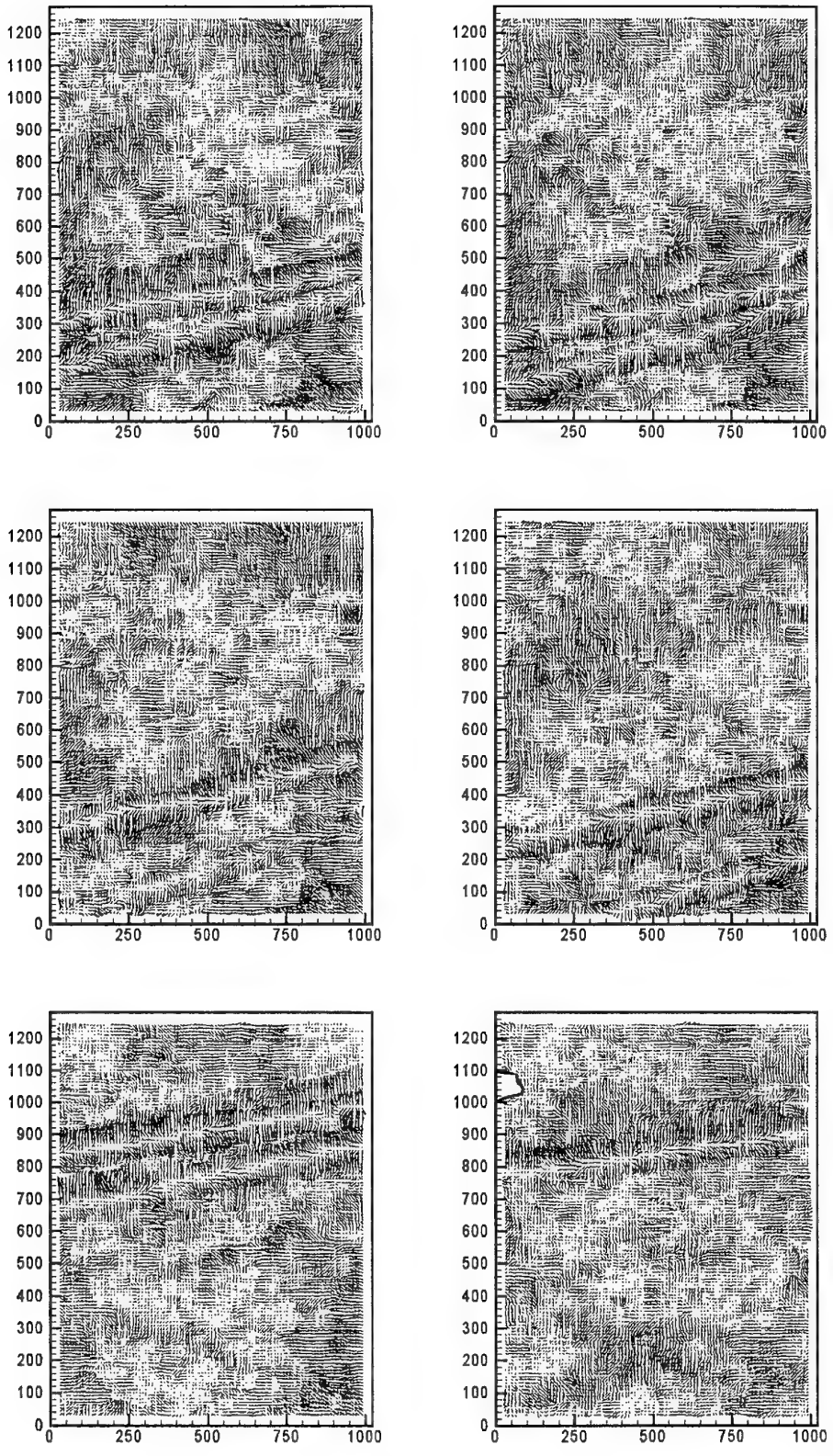

Fig. 40: Density gradient plots of further data samples

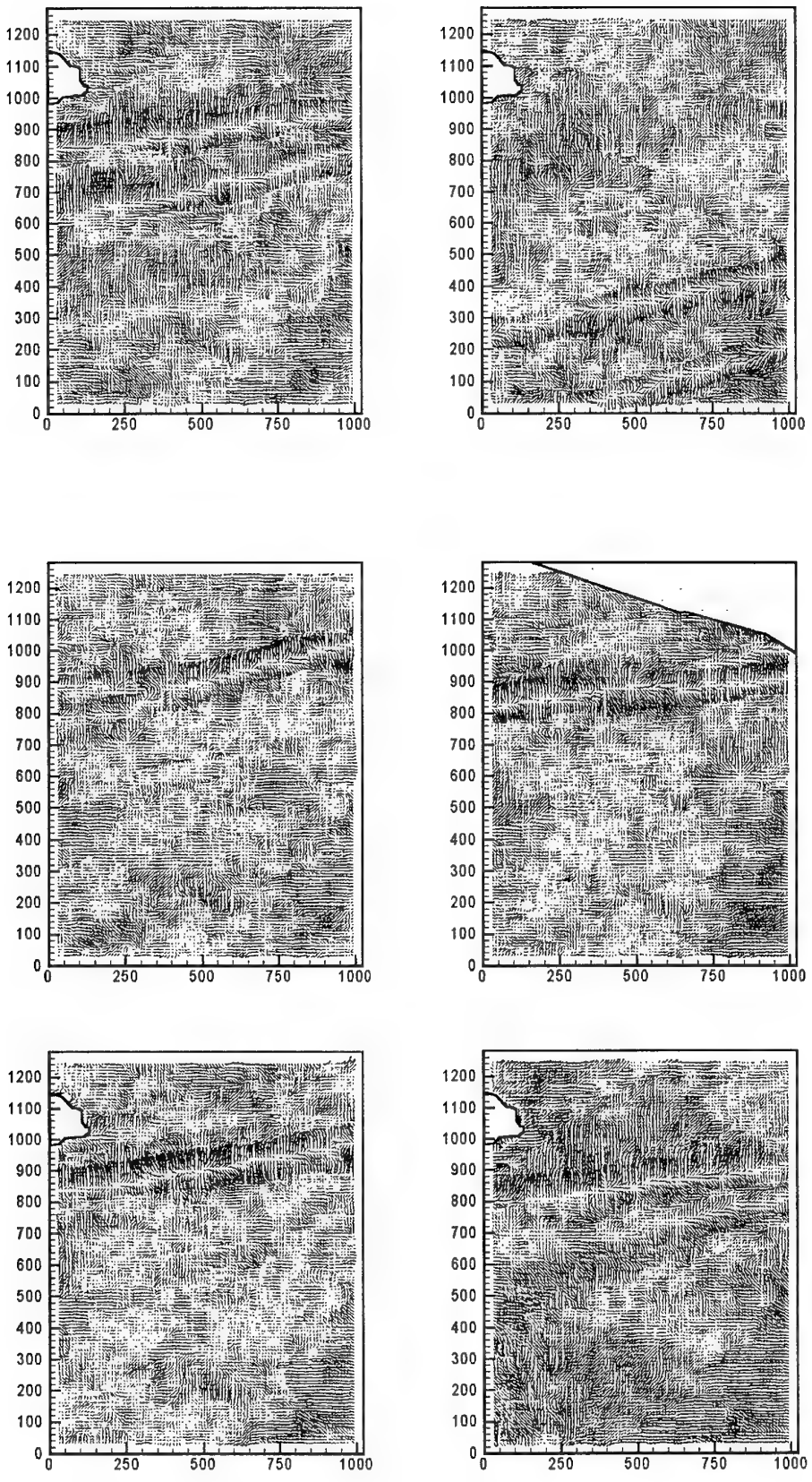

Fig. 41: Density gradient plots of further data samples

The formation of two individual vortices, rolling up to one larger vortex, the distance the vortices need to merge, and the radial position of the resulting vortex can clearly be identified on some of the above plots.

In the following recordings density gradients due to tip vortices as well as due to the turbine exhaust can be seen because helicopter had been turn by 90°.

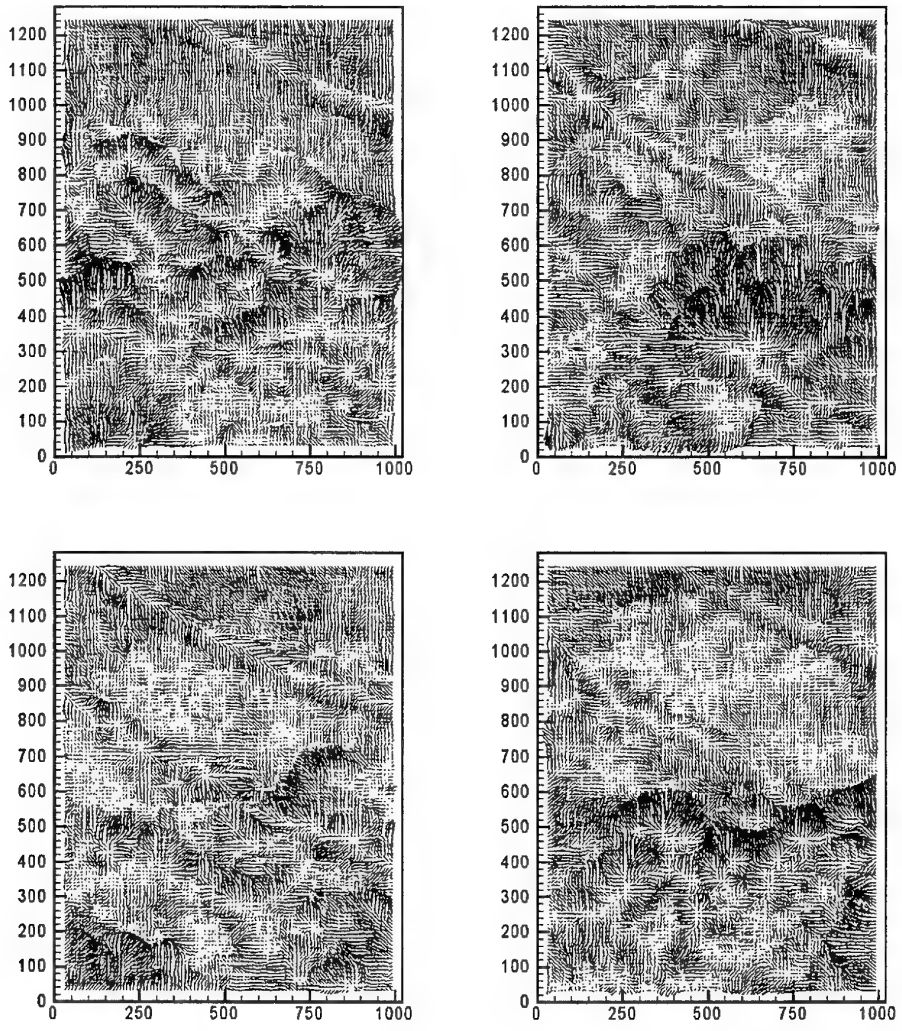

Fig. 42: Density gradient plots of data samples showing wing tip vortices together with the exhaust plume

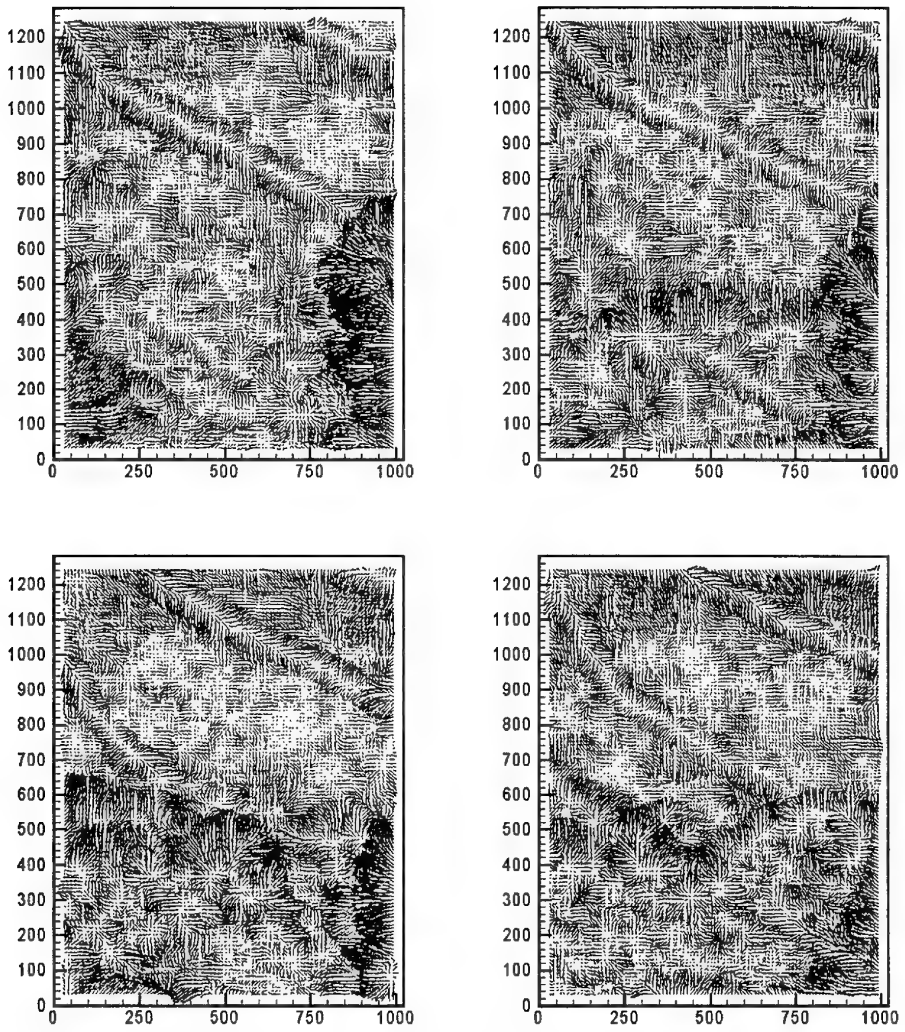

Fig. 43: Density gradient plots of data samples showing wing tip vortices together with the exhaust plume

The following recordings have been taken with another background. Instead of the dot pattern on the taxiway, we focused the cameras onto a grass patch between the taxiway and the runway. The results show, that such a background could be used for future investigations, which increases the chance to apply the technique in different flight conditions.

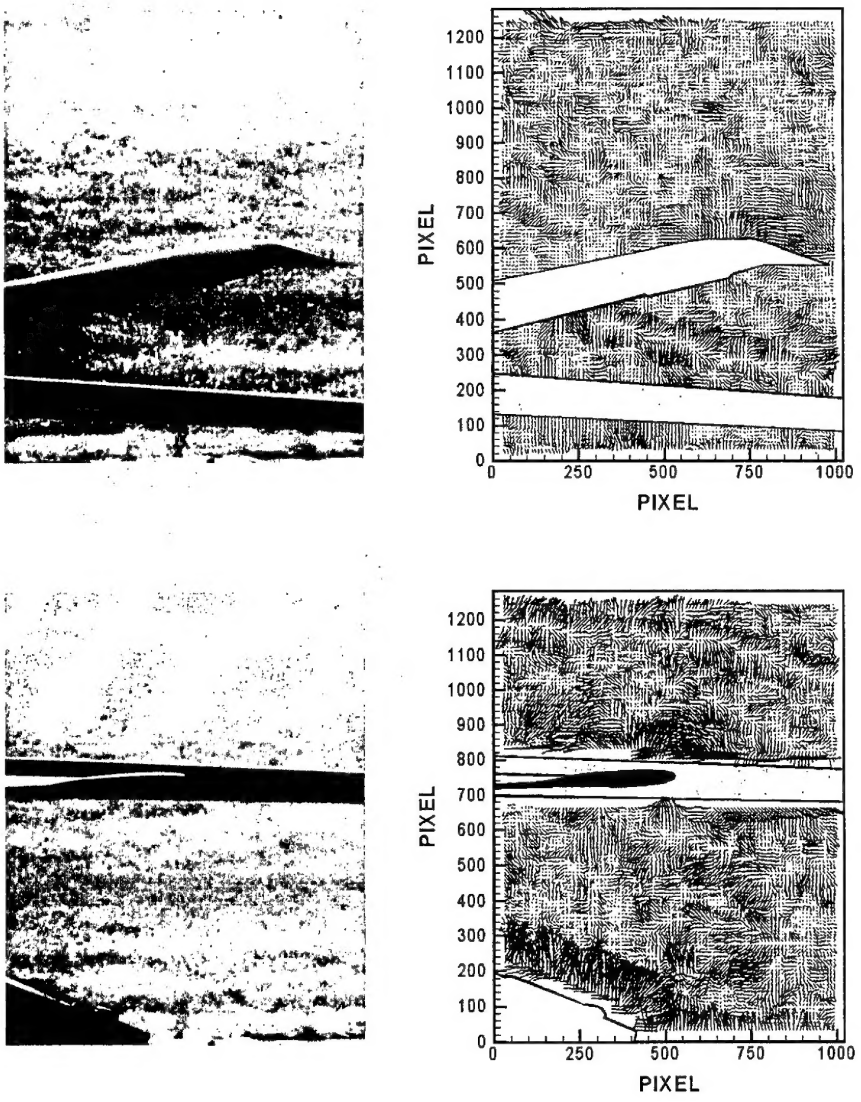

Fig. 44: Image data and density gradient plots of data samples showing wing tip vortices during decent flight conditions. The background used was a grass patch in approximately 100 meters distance from the cameras.

Discussion

Large scale flight tests with two helicopters confirmed the feasibility of the BOS and BOSS technique to visualize different blade tip vortices. It has been shown that geometric parameters like the location of the vortex relative to the rotor plane, orientation of the vortex axis in space, spatial information on vortex generation and roll up, and some information about the vortex size, can be derived. In spite of the difficult experimental conditions density gradient data were obtained, which allow to visualize density fields with encouraging spatial resolution. Compared to previous measurements the time needed for the setup and data acquisition can be considerably decreased in future. Future investigations have to be performed using multiple cameras in order to obtain more complete three-dimensional data.
After having demonstrated the feasibility of the concept by the application to a technological relevant but fluid mechanical quite complex problem, more detailed studies e.g. of tip vortices from stationary blades, could be performed in order to reduce the complexity of the flow structures under investigation.
However, the feasibility of using a 'natural background' like grass in a relative far background distance and the feasibility of the reference-free stereoscopic technique that enables the cameras to be mounted on board of the helicopter during future tests confirm the worthiness of the technique.

Acknowledgement

The authors would like to thank Ken McAlister, Alex Sheikman, J.T. Heineck and the people of the flight crew like Pilot Dave Arterburn at NASA Ames. Special thank also to the people at Nasa Langley for there help during the tests and for the fruitful discussions. The financial support of the ARL – European Research Office is greatly appreciated.

Literature

A. Bagai, J.G. Leishman: "Flow visualization of compressible vortex structures using density gradient techniques", *Exp. in Fluids*, Vol. 15, 431-442, 1993.

P. Beaumier, J. Prieur, G. Rahier, P. Spiegel, A. Demargne, R. Kube, B. van der Wall, B.G. Schultz, W. Splettstößer, C. Tung, J. Gallman, Y.H. Yu, T.F. Brooks, C.L. Burley, D.D. Boyd: "Effect of higher harmonic control on helicopter rotor blade vortex interaction noise", *75th Fluid Dynamics Symposium on Aerodynamics and Aeroacoustics of Rotorcraft,* Berlin, October 1994.

J.C. Biggers, K.L. Orloff: "Laser velocimeter measurements of the helicopter rotor induced flow field", *30th Annual National Forum of the American Helicopter Society*, reprint No. 800, May, 1974.

C.L. Burley, H.E. Jones, M.A. Marcolini, W.R. Splettstößer: "Directivity and prediction of low frequency rotor noise", *AIAA 91-0592, Aerospace Science Meeting, Reno*, USA 1991.

M.S. Chandrasekhara, D.D. Squires, M.C. Wilder, L.W. Carr: "A phase-locked high-speed real-time interferometry system for large amplitude unsteady flows", *7th International Symposium on Applications of Laser Techniques to Fluid Mechanics*, Lisbon, Portugal, 38.3.1-38.3.8, July, 1994.

S. Debrus, M. Francon, C.P. Grover, M. May, M.L. Robin: "Ground glass differential interferometer", *Applied Optics* 11, 853, 1972.

K. Ehrenfried, G.E.A. Meier, F. Obermeier: "Sound produced by vortex-airfoil interaction", *Proc. of the 17th European Rotorcraft Forum*, paper 63, Berlin, 1991.

G.T. Herman: "Image reconstruction from projections", Academic Press, New York, 1980.

U. Köpf: "Application of speckling for measuring the deflection of laser light by phase objects", *Optics Communications*, Vol. 5, No. 5, 347-350, 1972.

G.E.A. Meier: "New optical tools for fluid mechanics", *Proc. 8th International Symposium on Flow Visualization*, paper 226, Sorrento, Sept. 1998.

G.E.A. Meier, *9th International Symposium on Flow Visualization, Edinburgh*, August 22-25th 2000

M. Raffel, H. Richard, G.E.A. Meier: "On the applicability of background oriented optical tomography", *Experiments in Fluids 28 (2000)*, pp477-481

M. Raffel, U. Seelhorst, C. Willert: "Vortical flow structures at a helicopter rotor model measured by LDV and PIV", *Journal of the Royal Aeronautical Society*, 221-227, April, 1998.

M. Raffel, F. De Gregorio, K. Pengel, C. Willert, C. Kähler, T. Dewhirst, K. Ehrenfried, J. Kompenhans: "Instantaneous flow field measurements for propeller aircraft and rotorcraft research", *9th International Symposium on Applications of Laser Techniques to Fluid Mechanics*, Lisbon, Portugal, 19.6.1-19.6.8.10, (Bound volume in press), July, 1998.

M. Raffel, C. Willert, J. Kompenhans: "PIV A practical guide", *Springer Verlg*, April, 1998.

H.Richard, M. Raffel, M. Rein, J. Kompenhans, G.E.A. Meier: "Demonstration of the applicability of background oriented schlieren (BOS)", *Int. Symp. On Appl. Of Laser Techniques to Fluid Mechanics*, Lisbon, July 2000

O. Ronneberger, M. Raffel, J. Kompenhans: "Advanced evaluation algorithms for standard and dual plane particle image velocimetry", *9th International Symposium on Applications of Laser Techniques to Fluid Mechanics*, Lisbon, Portugal, 10.1.1-10.1.8, July, 1998.

R.H. Schlinker, R.K. Amiet: "Rotor vortex interaction noise", *NASA CR 3744*, Oct. 1983.

W.R. Splettstößer, K.J. Schultz, D.A. Boxwell, F.H. Schmitz: "Helicopter model rotor blade/vortex interaction impulsive noise: scalability and parametric variations", *NASA TM 86007*, 1984.

W.R. Splettstößer, R. Kube, W. Wagner, U. Seelhorst, A. Boutier, F. Micheli, E. Mercker, K. Pengel: "Key results from a higher harmonic control aeroacoustic rotor test (HART)", *Journal of the American Helicopter Society*, Vol. 42, No. 1, 58-78, 1997.

J.P. Sullivan: "An experimental investigation of vortex rings and helicopter rotor wakes using a laser Doppler velocimeter", MIT Technical Report 183, June. 1973.

J.L. Tangler: "Schlieren and noise studies of rotors in forward flight", *33rd Annual National Forum of the American Helicopter Society*, Reprint 77.33-05, May, 1977.

U. Wernekinck, W. Merzkirch: "Speckle photography of spatially extended refractive-index fields", *Applied Optics* Vol. 26, 31-32, 1987.